



HAL
open science

Design of Attribute EWMA Type Control Charts with Reliable Run Length Performance

Shu Wu, Philippe Castagliola, Athanasios Rakitzis, Petros Maravelakis

► **To cite this version:**

Shu Wu, Philippe Castagliola, Athanasios Rakitzis, Petros Maravelakis. Design of Attribute EWMA Type Control Charts with Reliable Run Length Performance. *Communications in Statistics - Simulation and Computation*, 2023, 52 (9), pp.4193-4209. 10.1080/03610918.2021.1955263 . hal-04225640

HAL Id: hal-04225640

<https://hal.science/hal-04225640>

Submitted on 3 Oct 2023

HAL is a multi-disciplinary open access archive for the deposit and dissemination of scientific research documents, whether they are published or not. The documents may come from teaching and research institutions in France or abroad, or from public or private research centers.

L'archive ouverte pluridisciplinaire **HAL**, est destinée au dépôt et à la diffusion de documents scientifiques de niveau recherche, publiés ou non, émanant des établissements d'enseignement et de recherche français ou étrangers, des laboratoires publics ou privés.

Design of Attribute EWMA Type Control Charts with Reliable Run Length Performance

Shu Wu^{1,2}, Philippe Castagliola^{*3}, Athanasios C. Rakitzis⁴
and Petros E. Maravelakis⁵

¹School of Logistics Engineering, Wuhan University of Technology,
Wuhan, China

²Engineering Research Center of Port Logistics Technology and
Equipment, Wuhan University of Technology, Wuhan, China

³Université de Nantes & LS2N UMR CNRS 6004, Nantes, France

⁴Department of Statistics and Actuarial-Financial Mathematics,
University of the Aegean, Karlovassi, Samos, Greece

⁵Department of Business Administration, University of Piraeus,
Piraeus, Greece

July 5, 2021

Abstract

Attribute control charts assuming a Poisson (c chart) or a binomial distribution (np chart) are usually used when the quality characteristic cannot be measured on a continuous scale. For equivalent sample sizes, Shewhart type attribute control charts are known to be less efficient than their measurement counterparts (like the \bar{X} chart) and, for this reason, practitioners often compensate it by supplementing them with an EWMA (Exponentially Weighted Moving Average) scheme. However, because of the discrete nature of count data, it is unfortunately impossible to compute exactly and accurately (by means of Markov chain of integral equation methods) the run length (RL) properties, such as its mean (ARL) and its standard deviation (SDRL) of these EWMA attribute control charts and, consequently, it is impossible to efficiently design them in order to minimize some out-of-control characteristics. For this reason, we propose in this paper a dedicated approach called “continuousify” method which, coupled with a classical Markov chain technique, allows to compute the RL properties of any EWMA attribute control chart in a reliable way. A numerical comparison shows that the RL properties obtained by using the proposed “continuousify” approach are very much alike to the ones calculated via simulation and without the “continuousify” approach. Illustrative examples are also provided to show how the proposed method can be implemented in practice.

*philippe.castagliola@univ-nantes.fr (corresponding author)

Keywords: Statistical Process Monitoring; Attribute EWMA chart; Markov chain; Normal mixture; Average Run Length; Poisson; Binomial.

1 Introduction

Statistical Process Monitoring (SPM) is a collection of statistical techniques providing a rational management of manufacturing processes, which allows high quality final products to be produced. Among SPM tools, the control charts are undeniably the ones that are the most used for identifying changes in processes. When the quality characteristic of interest can be measured, *measurement* type control charts (usually based on the normality assumption) are used (like the \bar{X} chart for the mean or the S chart for the standard-deviation) but, when this quality characteristic cannot be measured (and only defective / not defective products or number of defects can be observed), *attribute* type control charts (such as the c and np charts) are commonly used.

For comparable sample sizes, Shewhart type attribute control charts are known to be less efficient than their measurement counterparts and, for this reason, practitioners often compensate it by supplementing them with the EWMA (Exponentially Weighted Moving Average) scheme, introduced by Roberts (1959), which combines current and previous observations and is known to be one of the most effective tools for monitoring sustained changes in a process. Although EWMA type control charts have been massively studied in the case of normally distributed measurement data (among the most recent ones, we refer, for instance, to Khoo et al. (2016), Riaz and Abbasi (2016), Zwetsloot et al. (2016), Arshad et al. (2017), Bilen et al. (2017), Haridy et al. (2017), Lu and Huang (2017), Raji et al. (2018), Maravelakis et al. (2019) and Tang et al. (2019)), they have received less attention in the case of attribute data. For example, Gan (1990a,b) proposed modified EWMA control charts for monitoring Poisson and binomial counts, and he demonstrated that, based on the ARL (Average Run Length) criterion, these control charts are generally superior compared to the corresponding Shewhart control charts. Borrer et al. (1998) presented a methodology to design and evaluate the performance of the EWMA control chart for monitoring Poisson data and they found it more efficient than the Shewhart c chart and Gan (1990a)'s modified EWMA charts. Furthermore, other works concerning attribute EWMA control chart have been discussed by Somerville et al. (2002), Zhang et al. (2003), Yeh et al. (2008), Szarka and Woodall (2011), Saghir and Lin (2014), Aslam et al. (2018) and Alevizakos and Koukouvinos (2019).

In order to investigate the performance of a control chart, some in- and out-of-control RL (Run Length) properties have to be evaluated (for example, the ARL, MRL and SDRL) and accurate evaluation of these quantities is of great importance as they are often used in the design phase of a control chart. For example, for the design of an EWMA chart, the researcher has to find the optimal parameters $\lambda^* \in (0, 1]$ (smoothing parameter) and $K^* > 0$ (control limit parameter) such that, for a particular shift in the process, the out-of-control ARL is minimized subject to the constraint that the in-control ARL equals ARL_0 , a predefined value. If the evaluation of these RL properties is not reliable, it is

therefore hopeless to correctly design such a control chart. In the case of measurement data (usually, under the normality assumption) the RL properties of EWMA type control charts are obtained, in general, using either Markov chain or integral equation methods which are both based on a discretization of the control limits interval into m subintervals. When the number m of subintervals increases and becomes large enough (say $m \geq 200$) these methods yield fairly accurate approximations. On the other hand, in the case of attribute / count data, due to the discrete nature of these data, it is impossible to accurately compute any RL properties using Markov chain or integral equation methods as the results will heavily fluctuate depending on the value of the selected number m of subintervals (this will be clearly highlighted in the paper through some examples). Of course, it is always possible to obtain these values using Monte-Carlo simulations but, even in this case, if it is quite easy to compute small ARL or MRL values with some precision, it becomes just impossible to obtain reliable results when these values become very large. In addition, the design phase becomes significantly time consuming.

Therefore, in an attempt to extend the preliminary work by Wu et al. (2020), the goal of this paper is i) to propose a method, called “continuousify”, that allows to compute the RL properties of any attribute EWMA type control charts in a reliable way, ii) to demonstrate the use of this method in the case of the Poisson and binomial distributions, iii) to design the corresponding PEWMA (for Poisson EWMA) and BEWMA (for Binomial EWMA) and iv) to compare the results with the ones obtained through Monte Carlo simulations as well as with the ones presented in the very recent contribution of Morais and Knoth (2020) in which the authors tackle the same problem (for the PEWMA control chart only) but in a different way.

The paper is structured as follows. Section 2 introduces the “continuousify” technique as a general framework for discrete type distributions. Then, Section 3 focuses on two particular cases, i.e. the PEWMA control chart and the BEWMA control chart. In both cases, comparisons show how the “continuousify” technique allows to obtain stable and reliable ARL values. Moreover, we also provide the optimal values for the chart’s constants. In Section 4, two illustrative examples clarify how the “continuousify” approach can be used to monitor nonconformities or nonconforming items using EWMA. Finally, Section 5 summarizes the main findings and suggest potential new research directions.

2 The “continuousify” method for attribute type EWMA control charts

Let X_i , $i = 1, 2, \dots$, be a sequence of i.i.d. (independent and identically distributed) discrete r.v. (random variables), defined on $\Omega = \{\omega_1, \omega_2, \dots\}$ and having $f_X(\omega|\boldsymbol{\theta}) = P(X_i = \omega)$ as p.m.f. (probability mass function), where $\boldsymbol{\theta}$ is a vector of parameters. In practice, it is actually possible to define and implement an attribute EWMA type control chart directly monitoring a process (via the observed X_i values) by using the statistic $Z_i = \lambda X_i + (1 - \lambda)Z_{i-1}$,

$i = 1, 2, \dots$, where $\lambda \in (0, 1]$ is some smoothing parameter to be fixed and Z_0 is some initial value. As already explained in the Introduction section of this paper, the problem of this approach is that, because of the discrete nature of the r.v. X_i , $i = 1, 2, \dots$, it is impossible to accurately compute the RL properties of such a control chart (using Markov chain or integral equation methods) and, therefore, it is impossible to tune the chart parameters in order to obtain a predefined in-control performance. If, for instance, the Markov chain approach, (as detailed hereafter), is used in order to compute the ARL or the SDRL, the results will i) *heavily* fluctuate depending on the value of the selected number m of subintervals and ii) not exhibit any monotonic convergence when m increases, making useless such an approach. This point will be highlighted in Section 3.

Since the Markov chain and integral equation methods give good results in the case of *continuous* r.v., (and, more particularly in the case of the normal distribution, which is an unbounded one), we therefore suggest to transform each discrete r.v. X_i , $i = 1, 2, \dots$, into a new continuous one, denoted as X_i^* , (say that we “continuousify” the r.v. X_i), defined on $(-\infty, +\infty)$, and to monitor the process by using a traditional EWMA scheme. More precisely, we suggest to simply define X_i^* as a mixture of the r.v. $Y_{i,\omega_1}, Y_{i,\omega_2}, \dots$ where, for each $\omega \in \Omega$, $Y_{i,\omega} \sim N(\omega, \sigma)$, i.e.

$$X_i^* = \begin{cases} Y_{i,\omega_1} & \text{if } X_i = \omega_1, \\ Y_{i,\omega_2} & \text{if } X_i = \omega_2, \\ \vdots & \vdots \end{cases},$$

where $N(\omega, \sigma)$ stands for the Normal distribution with mean ω and standard deviation σ . Concretely speaking, this means that if, at $i = 1, 2, \dots$, we have $X_i = \omega \in \Omega$ then, in order to obtain X_i^* , we just have to generate a number from the $N(\omega, \sigma)$ distribution. The “continuousify” parameter $\sigma > 0$ has to be fixed and, as it will be shown later, its value does not significantly affect the performance of the control chart as long as it is neither too small nor too large. Since X_i^* , $i = 1, 2, \dots$, is defined as a mixture of normal distributions, its p.d.f. $f_{X^*}(x|\boldsymbol{\theta}, \sigma)$ and c.d.f. $F_{X^*}(x|\boldsymbol{\theta}, \sigma)$ are

$$f_{X^*}(x|\boldsymbol{\theta}, \sigma) = \sum_{\omega \in \Omega} f_X(\omega|\boldsymbol{\theta}) f_N(x|\omega, \sigma), \quad (1)$$

$$F_{X^*}(x|\boldsymbol{\theta}, \sigma) = \sum_{\omega \in \Omega} f_X(\omega|\boldsymbol{\theta}) F_N(x|\omega, \sigma), \quad (2)$$

where $f_N(x|\omega, \sigma)$ and $F_N(x|\omega, \sigma)$ are the p.d.f. and c.d.f. of the $N(\omega, \sigma)$ distribution, respectively. If $\mu = E(X)$ and $V(X)$ are the mean and variance of X_i , $i = 1, 2, \dots$, respectively, then it is not difficult to prove that the mean $\mu^* = E(X^*)$ and the variance $V(X^*)$ of X_i^* , $i = 1, 2, \dots$, are equal to (see Appendix for details):

$$E(X^*) = E(X), \quad (3)$$

$$V(X^*) = V(X) + \sigma^2. \quad (4)$$

In this paper, we will focus on an upper-sided EWMA control chart for process monitoring based on the statistic Z_i^* defined as

$$Z_i^* = \max(0, \lambda X_i^* + (1 - \lambda) Z_{i-1}^*), \quad (5)$$

with initial value $Z_0^* = \mu_0^*$ (corresponding to the in-control situation). Note that a similar approach can be used to design a lower-sided EWMA control chart properly modified. By definition, the asymptotic upper control limit UCL^* of this chart (i.e. with “continuously”) is equal to

$$\text{UCL}^* = \text{E}(X^*) + K \sqrt{\frac{\lambda}{2-\lambda}} \sqrt{\text{V}(X^*)},$$

where $K > 0$ is a control chart parameter to be fixed. Using (3) and (4), the previous formula simplifies to

$$\text{UCL}^* = \text{E}(X) + K \sqrt{\frac{\lambda(\text{V}(X) + \sigma^2)}{2-\lambda}}. \quad (6)$$

In order to obtain the zero-state ARL and SDRL of the proposed EWMA control chart, we suggest to use the standard approach proposed by Brook and Evans (1972). This approach assumes that the operation of this control chart can be well represented by a discrete-time Markov chain with $m + 2$ states. States $k \in \{0, 1, \dots, m\}$ are transient and state $m + 1$ is an absorbing one. The transition probability matrix \mathbf{P} of this discrete-time Markov chain is

$$\mathbf{P} = \begin{pmatrix} \mathbf{Q} & \mathbf{r} \\ \mathbf{0}^\top & 1 \end{pmatrix} = \begin{pmatrix} Q_{0,0} & Q_{0,1} & \cdots & Q_{0,m} & r_0 \\ Q_{1,0} & Q_{1,1} & \cdots & Q_{1,m} & r_1 \\ \vdots & \vdots & & \vdots & \vdots \\ Q_{m,0} & Q_{m,1} & \cdots & Q_{m,m} & r_m \\ 0 & 0 & \cdots & 0 & 1 \end{pmatrix},$$

where \mathbf{Q} is the $(m+1, m+1)$ matrix of transient probabilities, $\mathbf{0} = (0, 0, \dots, 0)^\top$ and the $(m+1, 1)$ vector \mathbf{r} satisfies $\mathbf{r} = \mathbf{1} - \mathbf{Q}\mathbf{1}$ (i.e. row probabilities must sum to 1) with $\mathbf{1} = (1, 1, \dots, 1)^\top$. The transient states $k \in \{1, \dots, m\}$ are obtained by dividing the interval $[0, \text{UCL}^*]$ into m subintervals of width 2Δ , where $\Delta = \frac{\text{UCL}^*}{2m}$ and UCL^* is the upper control limit as defined in (6). By definition, the midpoint of the k -th subinterval (representing state k) is equal to $H_k = (2k-1)\Delta$. The transient state $k = 0$ corresponds to the “restart state” feature of the upper-sided EWMA chart (due to the presence of the $\max(\dots)$ in (5)). This state is represented by the value $H_0 = 0$. It can be easily proven that the generic element $Q_{k,j}$, $k, j = 0, 1, \dots, m$, of the matrix \mathbf{Q} is equal to:

- if $j = 0$,

$$Q_{k,0} = F_{X^*} \left(-\frac{(1-\lambda)H_k}{\lambda} \middle| \boldsymbol{\theta}, \sigma \right),$$

- if $j = 1, 2, \dots, m$,

$$Q_{k,j} = F_{X^*} \left(\frac{H_j + \Delta - (1-\lambda)H_k}{\lambda} \middle| \boldsymbol{\theta}, \sigma \right) - F_{X^*} \left(\frac{H_j - \Delta - (1-\lambda)H_k}{\lambda} \middle| \boldsymbol{\theta}, \sigma \right),$$

where $F_{X^*}(\dots | \boldsymbol{\theta}, \sigma)$ is the c.d.f. of X_i^* , $i = 1, 2, \dots$, as defined in (2). Let $\mathbf{q} = (q_0, q_1, \dots, q_m)^\top$ be the $(m+1, 1)$ vector of initial probabilities associated with the $m+1$ transient states. In our case, we assume $\mathbf{q} = (1, 0, \dots, 0)^\top$, i.e. the initial state corresponds to the “restart state”. When the number m

of subintervals is sufficiently large (say $m \geq 200$), this approach provides an effective method that allows the ARL and SDRL to be accurately evaluated by using the following classical formulas from the theory of Markov chains (see, for instance Neuts (1981) or Latouche and Ramaswami (1999))

$$\begin{aligned} \text{ARL} &= \mathbf{q}^\top (\mathbf{I} - \mathbf{Q})^{-1} \mathbf{1}, \\ \text{SDRL} &= \sqrt{2\mathbf{q}^\top (\mathbf{I} - \mathbf{Q})^{-2} \mathbf{Q} \mathbf{1} + \text{ARL}(1 - \text{ARL})}. \end{aligned}$$

Of course, steady-state ARL and SDRL values can also be obtained by adequately modifying the vector \mathbf{q} of initial probabilities defined above. However, this topic is beyond the scope of this paper and we will not consider further the steady-state properties.

It has to be noted that the choice of the normal $N(\omega, \sigma)$ distribution in (1) and (2) for defining the mixture is just a possible choice among many others. In fact, in Perdakis et al. (2021), in a similar context, several symmetrical distributions / kernels (Normal, Parabolic, Biweight, Triweight, Cosine) have been tested and the conclusion was that the choice of the distribution / kernel clearly has almost no impact on the computation of the ARL and, therefore, the user is totally free to use the kernel / distribution of his / her choice (including the uniform distribution, for instance) without having to worry much about the reliability of the result.

3 Applications of the “continuousify” method

The goal of this section is to demonstrate the use of the “continuousify” method in the computation of the RL properties and the design of two upper-sided attribute EWMA control charts: the upper-sided PEWMA chart (assuming a Poisson distribution) and the upper-sided BEWMA chart (assuming a binomial distribution).

3.1 The “continuousified” upper-sided PEWMA chart

Let us assume that X_i , $i = 1, 2, \dots$ is a sequence of i.i.d. Poisson r.v. with parameter $\theta > 0$. When the process is in-control, we have $\theta = \theta_0$ and when the process is out-of-control, we have $\theta = \theta_1 > \theta_0$. In this case, we simply have $\boldsymbol{\theta} = \theta$, $\Omega = \{0, 1, 2, \dots\} = \mathbb{N}$, $f_X(\omega|\boldsymbol{\theta}) = \frac{e^{-\theta}\theta^\omega}{\omega!}$, $E(X^*) = \theta$, $V(X^*) = \theta + \sigma^2$ and the c.d.f. of X^* is equal to

$$F_{X^*}(x|\boldsymbol{\theta}, \sigma) = \sum_{\omega=0}^{+\infty} f_X(\omega|\boldsymbol{\theta}) F_N(x|\omega, \sigma).$$

The upper control limit UCL^* of the upper-sided PEWMA chart with the “continuousify” method is equal to

$$\text{UCL}^* = \theta_0 + K \sqrt{\frac{\lambda(\theta_0 + \sigma^2)}{2 - \lambda}}.$$

First of all, in order to have some insights about how to select the value of σ , we plotted in Figure 1 the p.d.f. $f_{X^*}(x|\boldsymbol{\theta}, \sigma)$ (i.e. using (1)) of the r.v. X^* for

$\theta = 3$ and for several values of $\sigma \in \{0.05, 0.1, 0.125, 0.15, 0.2, 0.4\}$. As it can be seen, if $\sigma = 0.05$, the resulting p.d.f. is too “peaky” and too close to the original discrete distribution, probably making the ARL values to still fluctuate a lot when the number of sub-intervals m varies. On the other hand, if $\sigma = 0.4$, the resulting p.d.f. is clearly too “over-smoothed”. In this case, the ARL values will not fluctuate any longer but, due to the term “ $\dots + \sigma^2$ ” in (6) these values will be larger. This will be confirmed in the following investigations. Therefore a good tradeoff seems to be a value for $\sigma \in [0.1, 0.2]$.

In Table 1 a comparison of the out-of-control ARL for the upper-sided PEWMA chart obtained *without* (left part) and *with* (right part) the “continuousify” method for a number of subintervals $m \in \{100, 110, \dots, 400\}$ and for the following out-of-control situations $(\theta_0, \theta_1) \in \{(1, 2), (1, 1.5), (2, 3), (4, 5), (4, 6)\}$ is given. For illustrative purposes, the control chart parameters are $K = 3$ and $\lambda = 0.2$ and the “continuousify” parameter is set at $\sigma = 0.125$ (this value has also been used in Wu et al. (2020)). As it can be seen (and as it was mentioned earlier):

- the ARL values obtained without “continuousify” heavily fluctuate (and they are sometimes even negative) depending on the value of m . Clearly, they do not exhibit any monotonic convergence when the number of subintervals m increases. For instance, in the case $(\theta_0, \theta_1) = (1, 1.5)$, the ARL values obtained without “continuousify” fluctuate from -82.8 (negative values may happen when the Markov chain approach does not converge) to 221.7 .
- on the contrary, for $m \geq 100$, the ARL values obtained with the “continuousify” method exhibit a *strong* stability and seem to converge rapidly to a reliable value. Even for $m = 100$ the results obtained with the “continuousify” approach are very reliable. This fact will reduce the time needed for the required computations for obtaining the RL distribution. For instance, using the same case $(\theta_0, \theta_1) = (1, 1.5)$, the ARL values obtained with “continuousify” converge rapidly to 28.4 .

As a matter of comparison, in Table 1, we have also computed the ARL values of the upper-sided PEWMA chart using 10^6 Monte-Carlo simulation runs (see bottom of Table 1) for the without “continuousify” case only. What can be seen is that the out-of-control ARL values obtained with the “continuousify” method (see for example the case $m = 400$), i.e. $9.9, 28.4, 17.3, 33.4, 10.2$ are almost the same or just a bit larger (in a negligible way) to the ones obtained using simulations without the “continuousify” method, i.e. $9.9, 28.3, 17.2, 33.4, 10.2$.

It is interesting to note that this topic (efficient ARL computation for EWMA control charts monitoring discrete data) has also grasped the attention of other researchers and, very recently, Morais and Knoth (2020) have proposed an alternative method called the “Splitting Markov Chain”. This approach has been applied to a two-sided PEWMA control chart (while, in this paper, we investigate a max-type upper sided PEWMA control chart). In order to compare the two methods, we have reproduced the three plots in Figure 3 page 880 of Morais and Knoth (2020), for the same two-sided PEWMA control charts, with the same settings (i.e. $(\lambda, K) \in \{(0.27, 3.3190), (0.57, 3.4598), (0.86, 3.4846)\}$)

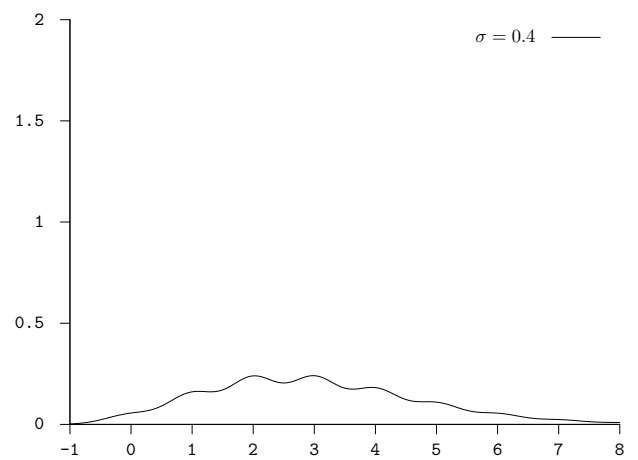
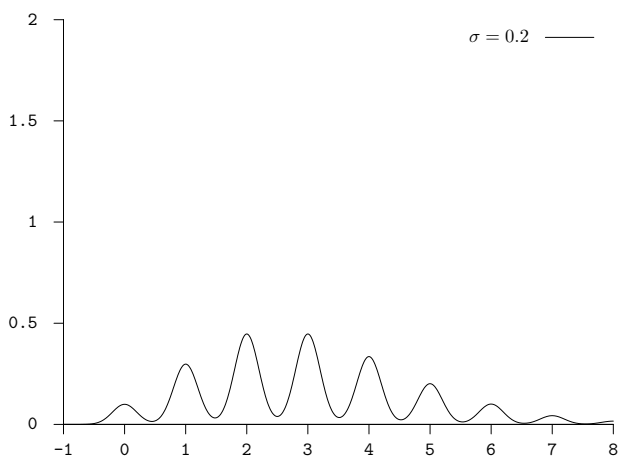
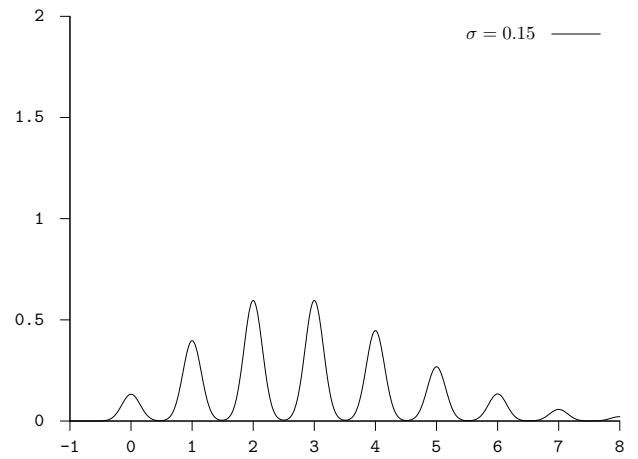
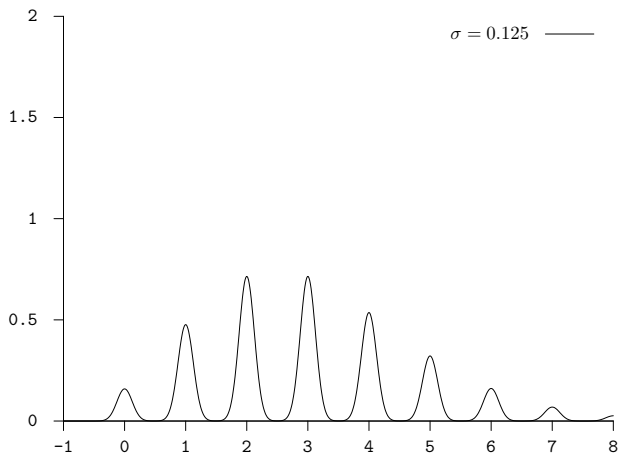
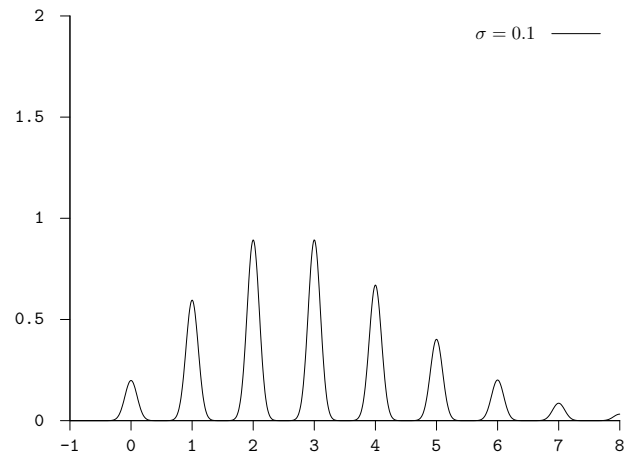
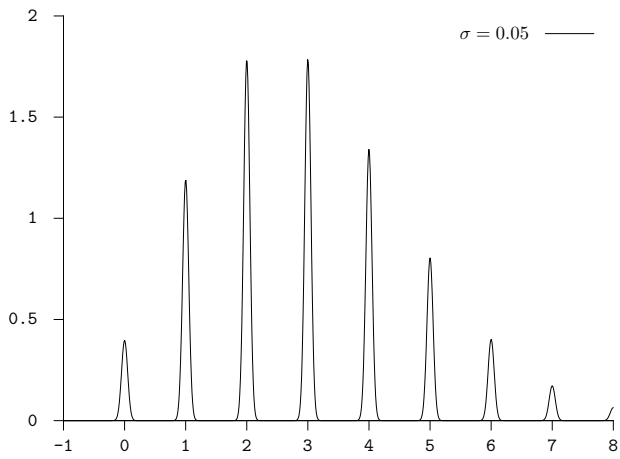


Figure 1: p.d.f. $f_{X^*}(x|\theta, \sigma)$ of X^* for $\theta = 3$ and $\sigma \in \{0.05, 0.1, 0.125, 0.15, 0.2, 0.4\}$

Table 1: Comparison of out-of-control ARL values for the upper-sided PEWMA chart obtained *with* and *without* “continuousify” when $K = 3$ and $\lambda = 0.2$

m	without “continuousify”					with “continuousify” ($\sigma = 0.125$)					
	$\theta_0 =$	1	2	4	4	$\theta_0 =$	1	2	4	4	
	$\theta_1 =$	2	1.5	3	5	6	$\theta_1 =$	2	1.5	3	5
100	10.9	56	17.2	105.8	11.9	9.9	28.4	17.3	33.5	10.2	
110	7.5	11.1	16	34.2	10.4	9.9	28.4	17.3	33.4	10.2	
120	7.1	10.3	17.5	-35.2	19	9.9	28.4	17.3	33.5	10.3	
130	8.3	14.7	18.5	27.1	10	9.9	28.4	17.3	33.5	10.2	
140	8.9	18.6	18.2	18.8	8.5	9.9	28.4	17.4	33.4	10.2	
150	8.3	17	18.1	10.5	6.9	9.9	28.4	17.3	33.5	10.3	
160	15.6	-82.8	17	20.1	8.8	9.9	28.4	17.3	33.5	10.2	
170	8.2	15.2	18	26.5	9.8	9.9	28.4	17.3	33.4	10.2	
180	8.9	18.5	16.4	19.9	9.1	9.9	28.4	17.3	33.5	10.3	
190	11.6	46.3	17.5	73.8	11.7	9.9	28.4	17.3	33.4	10.2	
200	7.2	12.1	16.3	22	8.9	9.9	28.4	17.3	33.4	10.2	
210	9	19.8	18.3	21.1	9	9.9	28.4	17.3	33.5	10.3	
220	15.8	-52.8	17.6	33.8	10.3	9.9	28.4	17.3	33.4	10.2	
230	7.3	12.8	17.3	63.8	11.1	9.9	28.4	17.3	33.4	10.2	
240	9.4	20.2	16.4	-45.1	15.2	9.9	28.4	17.3	33.5	10.2	
250	9.8	28	17.7	18	8.6	9.9	28.4	17.3	33.4	10.2	
260	9.2	21.1	16.5	32.8	9.8	9.9	28.4	17.3	33.4	10.2	
270	13	254	18	24.8	9.8	9.9	28.4	17.3	33.5	10.2	
280	8.3	19.3	17.7	432	13	9.9	28.4	17.3	33.4	10.2	
290	6.6	11.6	16.9	20.6	8.5	9.9	28.4	17.3	33.4	10.2	
300	15.4	-83.9	17.1	12.1	7.5	9.9	28.4	17.3	33.5	10.2	
310	8.2	14.2	17.3	41.7	10.6	9.9	28.4	17.3	33.4	10.2	
320	15.3	-50.1	15.2	345.7	12.8	9.9	28.4	17.3	33.4	10.2	
330	5.7	9.4	16.6	14.1	7.1	9.9	28.4	17.3	33.5	10.2	
340	9.2	21.2	16.9	30	9.9	9.9	28.4	17.3	33.4	10.2	
350	12.2	221.7	16.8	-298.7	13	9.9	28.4	17.3	33.4	10.2	
360	8.9	23.9	16.3	-16.4	26.2	9.9	28.4	17.3	33.5	10.2	
370	8.4	15.2	17.2	74.8	11.2	9.9	28.4	17.3	33.4	10.2	
380	6.3	10.3	18.3	20.4	8.8	9.9	28.4	17.3	33.4	10.2	
390	9.3	20.8	16.6	27.2	9.5	9.9	28.4	17.3	33.5	10.2	
400	7.2	10.7	17.5	122.1	12.1	9.9	28.4	17.3	33.4	10.2	
sim	9.9	28.3	17.2	33.4	10.2						

and the same scale, but using the “continuousify” approach instead of the “Splitting Markov Chain” approach. The corresponding plots are in Figure 2 where the three leftmost ones have been plotted for $\sigma = 0.125$ while the three rightmost ones have been plotted for $\sigma = 0.2$. From these plots, we can conclude that

- the results are *really* comparable to the ones in Morais and Knoth (2020). Fluctuations happen for some values $m < 100$ but, rapidly, when $m \geq 100$ the ARL values becomes stable.
- As expected, there are less fluctuations when $\sigma = 0.2$ rather than when $\sigma = 0.125$ but, as we already mentioned, the price to pay for this higher stability are larger ARL values as it can be noticed in the rightmost plots. Therefore a tradeoff has to be found and the value $\sigma = 0.125$ seems to be a good compromise.

As the “continuousify” method now provides stable values for the ARL it is therefore possible to design the upper-sided PEWMA chart in order to find the optimal parameters λ^* and K^* such that, for a particular shift from θ_0 to $\theta_1 = \tau\theta_0$, $\tau > 1$, the out-of-control ARL is minimized subject to the constraint that the in-control ARL equals the desired ARL_0 value, e.g. $ARL_0 = 370.4$. The optimal combinations (λ^*, K^*) are listed in Table 2 with the corresponding out-of-control ARL values for $\theta_0 \in \{1, 2, 5, 10\}$, $\tau \in \{1.1, 1.2, 1.5, 2, 3\}$ and $\sigma \in \{0.1, 0.125, 0.15, 0.2\}$. For instance, when $\theta_0 = 1$, $\tau = 2$ (i.e. $\theta_1 = 2$) and $\sigma = 0.1$, the optimal chart parameters are $(\lambda^*, K^*) = (0.115, 2.728)$ and the corresponding out-of-control ARL = 9.5. From Table 2, we can draw the following conclusions:

- No matter the value of σ , the out-of-control ARL values monotonically decrease when τ increases.
- The choice of the parameter $\sigma \in \{0.1, 0.125, 0.15, 0.2\}$ does not significantly impact the performance of the upper-sided PEWMA chart with “continuousify” as the difference in term of out-of-control ARL is almost negligible for a specified combination (θ_0, θ_1) . For example, if $\theta_0 = 2$ and $\tau = 1.1$ (i.e. $\theta_1 = 2.2$), the optimal parameters (λ^*, K^*) are approximately equal to $(0.03, 1.96)$, and the ARL values are approximately equal to 92, for the four possible choices of $\sigma \in \{0.1, 0.125, 0.15, 0.2\}$.

3.2 The upper-sided BEWMA chart with “continuousify”

Let us assume that X_i , $i = 1, 2, \dots$ is a sequence of i.i.d. binomial r.v. with parameters n and p . When the process is in-control, we have $p = p_0$ and when the process is out-of-control, we have $p = p_1 > p_0$. In this case, we have $\boldsymbol{\theta} = (n, p)$, $\Omega = \{0, 1, 2, \dots, n\}$, $f_X(\omega|\boldsymbol{\theta}) = \binom{n}{\omega} p^\omega (1-p)^{n-\omega}$, $E(X^*) = np$, $V(X^*) = np(1-p) + \sigma^2$ and the c.d.f. of X^* is equal to

$$F_{X^*}(x|\boldsymbol{\theta}, \sigma) = \sum_{\omega=0}^n f_X(\omega|\boldsymbol{\theta}) F_N(x|\omega, \sigma).$$

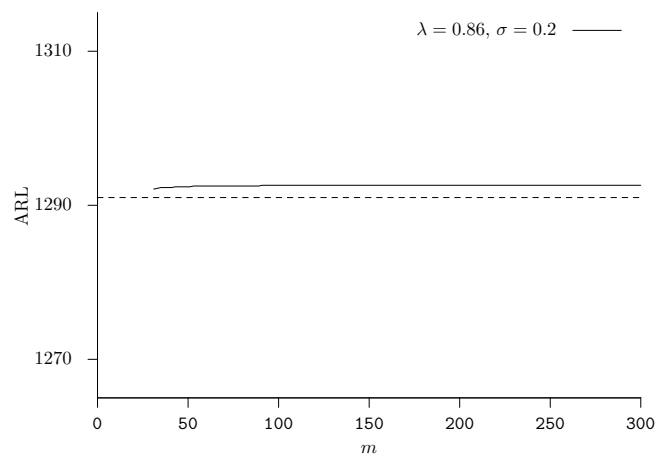
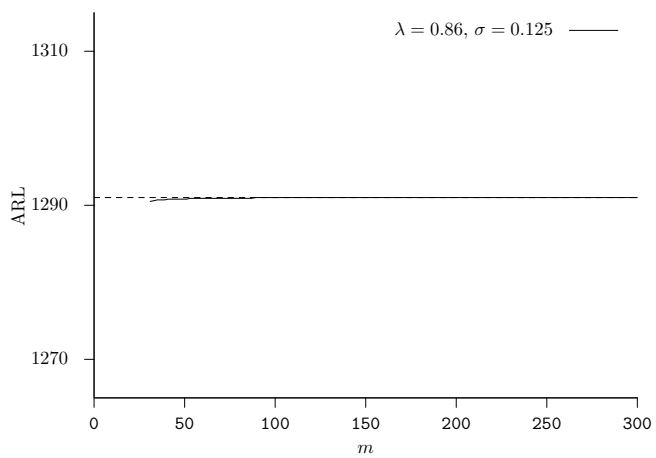
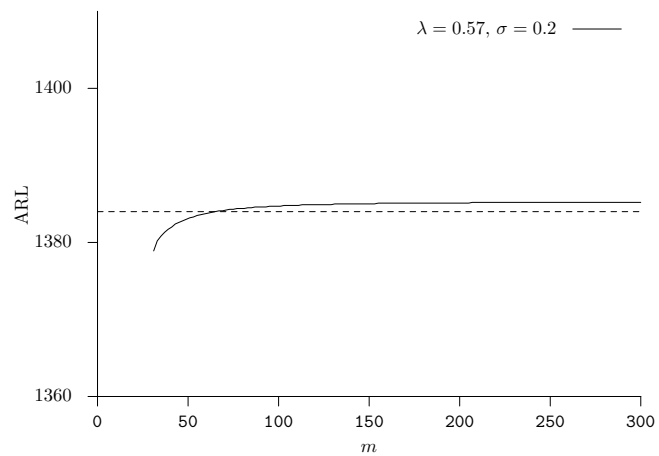
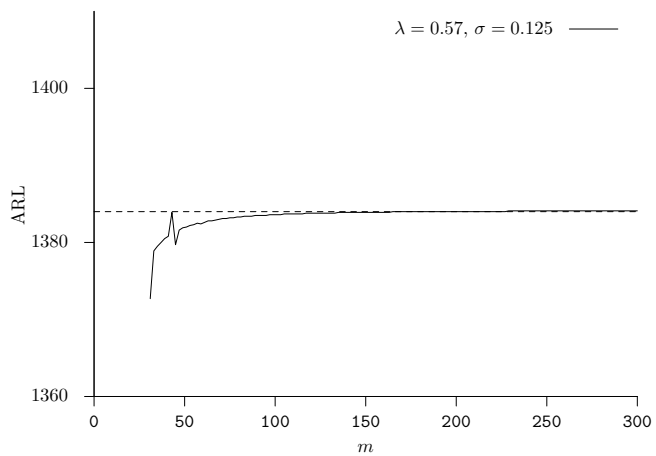
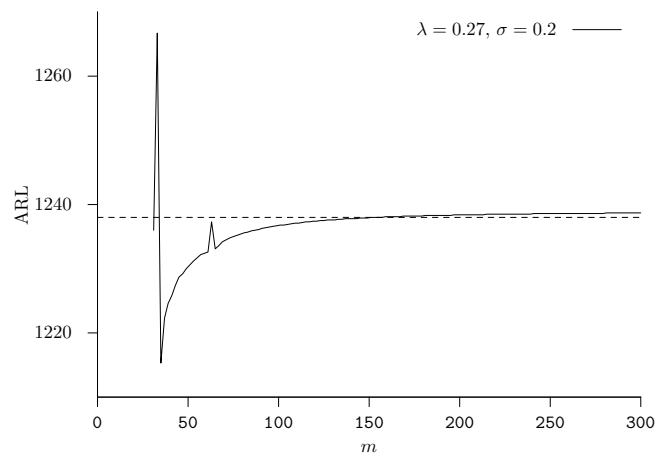
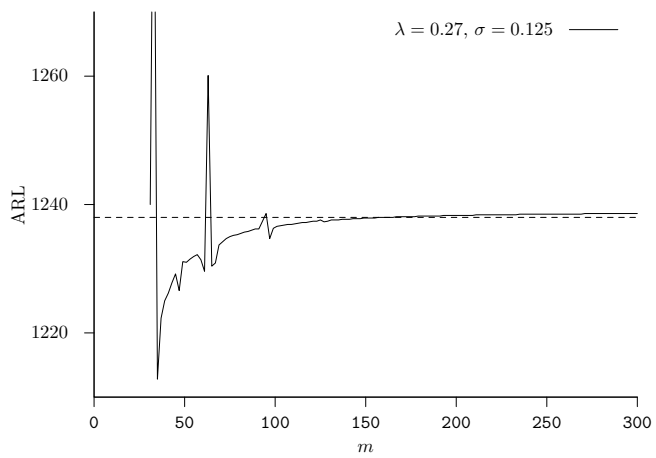


Figure 2: Comparison with the plots in Figure 3 page 880 in Morais and Knoth (2020)

Table 2: Optimal combinations (λ^*, K^*) and corresponding out-of-control ARL values for $\theta_0 \in \{1, 2, 5, 10\}$, $\tau \in \{1.1, 1.2, 1.5, 2, 3\}$ and $\sigma \in \{0.1, 0.125, 0.15, 0.2\}$ for the upper-sided PEWMA chart with “continuousify”

θ_0	τ	θ_1	$\sigma = 0.1$	$\sigma = 0.125$	$\sigma = 0.15$	$\sigma = 0.2$
1	1.1	1.1	(0.030, 1.986, 126.6)	(0.030, 1.985, 126.8)	(0.030, 1.984, 127.0)	(0.030, 1.983, 127.6)
	1.2	1.2	(0.030, 1.986, 64.2)	(0.030, 1.985, 64.3)	(0.030, 1.984, 64.4)	(0.030, 1.983, 64.8)
	1.5	1.5	(0.035, 2.077, 22.4)	(0.035, 2.076, 22.4)	(0.035, 2.075, 22.5)	(0.035, 2.072, 22.6)
	2	2	(0.115, 2.728, 9.5)	(0.115, 2.725, 9.6)	(0.115, 2.722, 9.5)	(0.120, 2.737, 9.6)
	3	3	(0.260, 3.144, 4.0)	(0.245, 3.108, 4.0)	(0.265, 3.147, 4.0)	(0.250, 3.106, 4.0)
2	1.1	2.2	(0.030, 1.965, 92.0)	(0.030, 1.964, 92.1)	(0.030, 1.964, 92.2)	(0.030, 1.963, 92.5)
	1.2	2.4	(0.030, 1.965, 43.0)	(0.030, 1.964, 43.1)	(0.030, 1.964, 43.1)	(0.030, 1.963, 43.2)
	1.5	3	(0.075, 2.446, 14.2)	(0.080, 2.476, 14.3)	(0.080, 2.475, 14.3)	(0.080, 2.473, 14.4)
	2	4	(0.210, 2.920, 5.8)	(0.215, 2.929, 5.8)	(0.215, 2.927, 5.8)	(0.185, 2.856, 5.8)
	3	6	(0.375, 3.163, 2.4)	(0.385, 3.173, 2.4)	(0.385, 3.171, 2.4)	(0.395, 3.177, 2.4)
5	1.1	5.5	(0.030, 2.060, 55.3)	(0.030, 2.044, 55.6)	(0.030, 2.027, 55.9)	(0.030, 2.004, 55.1)
	1.2	6	(0.035, 2.031, 24.7)	(0.035, 2.031, 24.7)	(0.035, 2.031, 24.7)	(0.030, 2.004, 24.7)
	1.5	7.5	(0.150, 2.683, 7.5)	(0.150, 2.682, 7.5)	(0.150, 2.682, 7.5)	(0.155, 2.693, 7.6)
	2	10	(0.345, 2.978, 3.0)	(0.355, 2.987, 3.0)	(0.355, 2.987, 3.0)	(0.355, 2.986, 3.0)
	3	15	(0.585, 3.143, 1.3)	(0.595, 3.147, 1.3)	(0.610, 3.152, 1.3)	(0.640, 3.163, 1.3)
10	1.1	11	(0.035, 2.025, 37.3)	(0.035, 2.025, 37.4)	(0.035, 2.025, 37.4)	(0.035, 2.025, 37.4)
	1.2	12	(0.055, 2.199, 15.7)	(0.055, 2.203, 15.7)	(0.075, 2.372, 15.8)	(0.075, 2.371, 15.8)
	1.5	15	(0.285, 2.846, 4.6)	(0.275, 2.836, 4.6)	(0.275, 2.836, 4.6)	(0.275, 2.835, 4.6)
	2	20	(0.530, 3.013, 1.8)	(0.530, 3.012, 1.8)	(0.545, 3.018, 1.8)	(0.545, 3.018, 1.8)
	3	30	(0.890, 3.113, 1.0)	(0.890, 3.112, 1.0)	(0.890, 3.112, 1.0)	(0.890, 3.110, 1.0)

The upper control limit UCL^* of the upper-sided BEWMA chart with the “continuousify” method is equal to

$$UCL^* = np_0 + K \sqrt{\frac{\lambda(np_0(1-p_0) + \sigma^2)}{2-\lambda}}.$$

Similarly to Table 1, Table 3 compares the out-of-control ARL of the upper-sided BEWMA chart obtained *without* (left part) and *with* (right part) the “continuousify” method for a number of subintervals $m \in \{100, 110, \dots, 400\}$ and for the following out-of-control situations $(n, p_0, p_1) = \{(40, 0.05, 0.06), (20, 0.1, 0.12), (10, 0.1, 0.15), (20, 0.15, 0.18), (10, 0.15, 0.2)\}$. As for Table 1, the control chart parameters are $K = 3$ and $\lambda = 0.2$ and the “continuousify” parameter is set at $\sigma = 0.125$. As it can be seen, the conclusions drawn for the upper-sided PEWMA chart can also be drawn for the upper-sided BEWMA chart, i.e. i) the ARL values obtained without “continuousify” heavily fluctuate and they clearly do not exhibit any monotonic convergence when the number of subintervals m increases, ii) on the contrary, for $m \geq 100$, the ARL values obtained with the “continuousify” method exhibit a *strong* stability and seem to converge rapidly to a reliable value, iii) the ARL values obtained with the “continuousify” method (see for example the case $m = 400$ with 74.1, 74.5, 27.8, 57.2, 39.9) are a bit larger (again in a negligible way) than the ones obtained by simulations without the “continuousify” method, i.e. 73.6, 73.5, 27.4, 56.6, 39.4.

As the “continuousify” method also provides stable and reliable ARL values for the upper-sided BEWMA chart, it is therefore possible to design it in or-

Table 3: Comparison of out-of-control ARL values for the upper-sided BEWMA chart obtained *with* and *without* “continuousify” when $K = 3$ and $\lambda = 0.2$

	without “continuousify”					with “continuousify” ($\sigma = 0.125$)				
	$n = 40$	20	10	20	10	$n = 40$	20	10	20	10
$p_0 =$	0.05	0.1	0.1	0.15	0.15	$p_0 =$ 0.05	0.1	0.1	0.15	0.15
$p_1 =$	0.06	0.12	0.15	0.18	0.2	$p_1 =$ 0.06	0.12	0.15	0.18	0.2
100	94.3	52.4	25.2	52.8	55.9	74.0	74.4	27.8	57.0	39.9
110	146.4	51.6	30.4	68.9	44.9	74.0	74.4	27.8	57.2	39.9
120	43.6	71.2	46.8	56.1	32.3	74.2	74.4	27.8	57.1	39.8
130	81.7	114.1	23.7	52.6	30.4	74.1	74.4	27.8	57.2	39.9
140	49.0	70.6	22.1	54.1	59.6	74.1	74.4	27.9	57.1	39.9
150	59.3	100.7	26.7	63.0	38.5	74.1	74.4	27.9	57.2	39.8
160	78.4	189.0	19.6	60.8	31.9	74.1	74.4	27.9	57.1	39.8
170	79.6	87.8	42.6	53.0	62.8	74.1	74.4	27.9	57.2	39.9
180	67.0	74.3	24.5	51.1	39.3	74.1	74.4	27.9	57.1	39.9
190	58.4	62.7	32.8	52.9	32.2	74.1	74.4	27.8	57.2	39.8
200	83.4	70.3	35.4	54.9	53.2	74.1	74.4	27.8	57.1	39.9
210	62.1	68.2	29.0	59.5	47.8	74.1	74.4	27.8	57.2	39.9
220	70.3	60.7	21.1	59.8	30.6	74.1	74.4	27.8	57.1	39.8
230	84.1	67.3	35.7	50.9	38.1	74.1	74.4	27.9	57.2	39.9
240	45.1	85.4	60.0	51.3	32.2	74.1	74.4	27.9	57.2	39.9
m 250	60.6	121.3	48.6	55.0	29.2	74.1	74.4	27.9	57.2	39.8
260	52.4	75.6	33.0	63.1	34.0	74.1	74.4	27.9	57.2	39.9
270	78.0	55.7	24.5	62.4	29.8	74.1	74.4	27.9	57.1	39.9
280	85.2	73.9	40.5	60.0	34.3	74.1	74.4	27.8	57.2	39.9
290	82.5	63.9	23.8	52.0	38.5	74.1	74.4	27.8	57.1	39.8
300	57.9	90.6	27.5	60.5	61.5	74.1	74.4	27.8	57.2	39.9
310	191.6	61.4	19.8	62.3	30.3	74.1	74.4	27.8	57.1	39.9
320	129.5	127.7	24.6	60.6	88.1	74.1	74.4	27.8	57.2	39.8
330	81.3	62.9	29.9	64.9	29.0	74.1	74.4	27.9	57.1	39.9
340	90.5	72.5	37.8	55.7	28.1	74.1	74.4	27.9	57.2	39.9
350	70.1	80.2	27.6	54.3	38.4	74.1	74.4	27.9	57.1	39.9
360	61.8	68.1	42.3	59.8	29.7	74.1	74.4	27.9	57.2	39.9
370	74.9	72.5	34.7	51.2	56.6	74.1	74.4	27.8	57.1	39.9
380	51.6	118.7	32.8	60.0	50.6	74.1	74.4	27.8	57.2	39.9
390	60.0	74.9	20.1	57.5	33.4	74.1	74.4	27.8	57.1	39.9
400	83.4	63.4	25.4	56.0	38.8	74.1	74.5	27.8	57.2	39.9
sim	73.6	73.5	27.4	56.6	39.4					

der to find the optimal parameters λ^* and K^* such that, for a particular shift from p_0 to $p_1 = \tau p_0$, $\tau \in (1, 1/p_0)$, the out-of-control ARL is minimized under the constraint that the in-control ARL = ARL₀ = 370.4. The optimal combinations (λ^*, K^*) are listed in Table 4 with the corresponding out-of-control ARL values for $p_0 \in \{0.05, 0.1, 0.15, 0.2\}$, $\tau \in \{1.1, 1.2, 1.5, 2, 3\}$ and $\sigma \in \{0.1, 0.125, 0.15, 0.2\}$. For instance, when $p_0 = 0.1$, $\tau = 1.2$ (i.e. $p_1 = 0.12$), $n = 20$ and $\sigma = 0.15$, the optimal chart parameters are $(\lambda^*, K^*) = (0.030, 1.954)$ and the corresponding out-of-control ARL = 40.7. As for the upper-sided PEWMA chart, similar conclusions can be drawn from Table 4 for the the upper-sided BEWMA chart, i.e. i) no matter the value of σ , the out-of-control ARL values monotonically decrease when τ increases and ii) for a specified combination (p_0, p_1) , the choice of $\sigma \in \{0.1, 0.125, 0.15, 0.2\}$ does not significantly impact the performance of the upper-sided BEWMA chart with “continuousify” in terms of the out-of-control ARL. For instance, for the four possible values of $\sigma \in \{0.1, 0.125, 0.15, 0.2\}$, if $p_0 = 0.1$, $p_1 = 0.12$ and $n = 20$, then the optimal parameters (λ^*, K^*) are approximately equal to $(0.03, 1.96)$ and the out-of-control ARL values range from 39.9 to 40.8.

4 Illustrative examples

4.1 Example of an upper-sided PEWMA chart with “continuousify”

This example is based on the data provided in Chapter 7 of Montgomery (2013) (Tables 7.7 and 7.8). These tables present the number of nonconformities observed in 44 (initially, they were 46 samples but two of them have been proved to be out-of-control) successive samples of 100 printed circuit boards. The data set is divided into two subsets: the first 24 samples are used as a Phase I data set and the remaining 20 samples are used as a Phase II data set (see column X_i in Table 5).

Using the Phase I data, the in-control number of nonconformities per sample is estimated as $\hat{\theta}_0 = \frac{472}{24} = 19.67$. Assuming $K = 3$, $\lambda = 0.2$ and $\sigma = 0.125$, the upper control limit UCL* of the upper-sided PEWMA chart with the “continuousify” method is equal to

$$\text{UCL}^* = 19.67 + 3 \times \sqrt{\frac{0.2 \times (19.67 + 0.125^2)}{2 - 0.2}} = 24.103.$$

Note that without the “continuousify” method (i.e. $\sigma = 0$) this upper control limit would have been UCL = 24.101 which is almost the same as for the with “continuousify” approach.

In addition to the number of nonconformities X_i , Table 5 also lists the values of X_i^* , Z_i (based on X_i) and Z_i^* for Phases I and II. These Phases have been treated separately with initial values $Z_0 = Z_0^* = 19.67$. As it can be seen the values of Z_i (without “continuousify”) are actually different but nevertheless very close to those of Z_i^* (with “continuousify”). This highlights the fact that the “continuousify” technique has a very small impact in the computation of the EWMA statistic itself (but it has a positive strong impact in the computation of

Table 4: Optimal combinations (λ^*, K^*) and corresponding out-of-control ARL values for $p_0 \in \{0.05, 0.1, 0.15, 0.2\}$, $\tau \in \{1.1, 1.2, 1.5, 2\}$ and $\sigma \in \{0.1, 0.125, 0.15, 0.2\}$ for the upper-sided BEWMA chart with “continuousify”

p_0	τ	p_1	$\sigma = 0.1$			$\sigma = 0.125$				
			$n = 10$	$n = 20$	$n = 50$	$n = 100$	$n = 10$	$n = 20$	$n = 50$	$n = 100$
0.05	1.1	0.055	(0.030, 2.013, 162.2)	(0.030, 1.981, 123.8)	(0.030, 1.975, 79.7)	(0.030, 2.063, 54.4)	(0.030, 2.011, 162.6)	(0.030, 1.980, 124.0)	(0.030, 1.966, 80.0)	(0.030, 2.052, 53.2)
	1.2	0.06	(0.030, 2.013, 90.5)	(0.030, 1.981, 62.2)	(0.030, 1.975, 36.5)	(0.030, 2.152, 23.8)	(0.030, 2.011, 90.9)	(0.030, 1.980, 62.3)	(0.030, 1.966, 36.6)	(0.030, 2.052, 23.8)
	1.5	0.075	(0.030, 2.013, 33.0)	(0.030, 2.070, 21.6)	(0.030, 2.530, 11.8)	(0.045, 2.657, 7.2)	(0.030, 2.011, 33.2)	(0.030, 2.069, 21.7)	(0.030, 2.529, 11.8)	(0.045, 2.657, 7.2)
	2	0.1	(0.070, 2.513, 14.6)	(0.125, 2.746, 9.1)	(0.220, 2.877, 4.7)	(0.470, 3.049, 2.8)	(0.060, 2.422, 14.4)	(0.120, 2.723, 9.1)	(0.220, 2.877, 4.7)	(0.470, 3.048, 2.8)
	1.1	0.11	(0.030, 1.975, 120.9)	(0.030, 1.960, 86.6)	(0.030, 2.069, 51.8)	(0.030, 1.938, 35.3)	(0.030, 1.974, 121.1)	(0.030, 1.958, 86.6)	(0.030, 2.050, 52.1)	(0.030, 2.023, 34.6)
	1.2	0.12	(0.030, 1.975, 60.2)	(0.030, 1.960, 39.9)	(0.030, 2.196, 23.0)	(0.055, 2.184, 14.7)	(0.030, 1.974, 60.4)	(0.030, 1.958, 39.9)	(0.030, 2.196, 23.0)	(0.055, 2.189, 14.7)
0.1	1.5	0.15	(0.035, 2.063, 20.8)	(0.070, 2.391, 13.2)	(0.170, 2.701, 6.9)	(0.315, 2.844, 4.2)	(0.035, 2.063, 20.9)	(0.070, 2.391, 13.2)	(0.170, 2.701, 6.9)	(0.315, 2.844, 4.2)
	2	0.2	(0.120, 2.701, 8.6)	(0.245, 2.925, 5.3)	(0.405, 2.976, 2.7)	(0.595, 2.990, 1.6)	(0.120, 2.699, 8.7)	(0.225, 2.891, 5.3)	(0.430, 2.993, 1.6)	(0.615, 2.996, 1.6)
	1.1	0.165	(0.030, 1.960, 97.4)	(0.030, 1.949, 67.6)	(0.030, 1.947, 39.6)	(0.030, 1.948, 26.4)	(0.030, 1.959, 97.5)	(0.030, 1.948, 67.7)	(0.030, 1.947, 39.6)	(0.030, 1.949, 26.4)
	1.2	0.18	(0.030, 1.960, 45.8)	(0.030, 1.949, 30.2)	(0.065, 2.304, 17.0)	(0.125, 2.536, 10.6)	(0.030, 1.959, 45.9)	(0.030, 1.948, 30.3)	(0.065, 2.303, 17.0)	(0.125, 2.536, 10.6)
	1.5	0.225	(0.080, 2.448, 15.3)	(0.130, 2.616, 9.5)	(0.265, 2.799, 4.9)	(0.385, 2.847, 3.0)	(0.080, 2.448, 15.3)	(0.130, 2.616, 9.5)	(0.265, 2.799, 4.9)	(0.400, 2.855, 3.0)
	2	0.3	(0.190, 2.828, 6.1)	(0.265, 2.873, 3.7)	(0.575, 2.986, 1.9)	(0.795, 2.969, 1.2)	(0.190, 2.826, 6.1)	(0.265, 2.872, 3.7)	(0.590, 2.991, 1.9)	(0.815, 2.971, 1.2)
0.2	1.1	0.22	(0.030, 1.949, 81.9)	(0.030, 1.942, 56.0)	(0.030, 1.935, 32.5)	(0.050, 2.169, 21.1)	(0.030, 1.948, 82.0)	(0.030, 1.941, 56.1)	(0.030, 1.936, 32.5)	(0.050, 2.170, 21.1)
	1.2	0.24	(0.030, 1.949, 37.4)	(0.040, 2.090, 24.6)	(0.090, 2.423, 13.5)	(0.175, 2.625, 8.3)	(0.030, 1.948, 37.4)	(0.040, 2.089, 24.6)	(0.090, 2.422, 13.5)	(0.175, 2.625, 8.3)
	1.5	0.3	(0.090, 2.478, 12.0)	(0.165, 2.673, 7.4)	(0.325, 2.817, 3.8)	(0.560, 2.881, 2.2)	(0.090, 2.477, 12.0)	(0.165, 2.673, 7.4)	(0.325, 2.816, 3.8)	(0.560, 2.881, 2.3)
	2	0.4	(0.245, 2.856, 4.7)	(0.350, 2.900, 2.8)	(0.695, 2.959, 1.4)	(0.890, 2.933, 1.0)	(0.245, 2.855, 4.7)	(0.360, 2.906, 2.8)	(0.715, 2.964, 1.4)	(0.890, 2.933, 1.0)
	1.1	0.165	(0.030, 1.954, 121.4)	(0.030, 1.954, 87.9)	(0.030, 2.030, 52.4)	(0.035, 2.023, 34.7)	(0.030, 1.969, 122.8)	(0.030, 1.953, 88.1)	(0.030, 1.996, 53.0)	(0.035, 2.021, 34.7)
	1.2	0.12	(0.030, 1.974, 60.5)	(0.030, 1.954, 40.7)	(0.035, 2.025, 23.2)	(0.055, 2.194, 14.7)	(0.030, 1.969, 61.5)	(0.030, 1.953, 40.8)	(0.035, 2.024, 23.2)	(0.055, 2.361, 14.8)
0.15	1.5	0.15	(0.030, 1.974, 20.9)	(0.070, 2.390, 13.2)	(0.170, 2.701, 6.9)	(0.315, 2.843, 4.2)	(0.045, 2.197, 21.1)	(0.075, 2.420, 13.3)	(0.170, 2.700, 6.9)	(0.315, 2.843, 4.2)
	2	0.2	(0.130, 2.733, 8.7)	(0.225, 2.889, 5.3)	(0.430, 2.992, 2.7)	(0.615, 2.996, 1.6)	(0.115, 2.670, 8.8)	(0.230, 2.893, 5.3)	(0.440, 2.997, 2.7)	(0.630, 3.000, 1.6)
	1.1	0.165	(0.030, 1.957, 97.6)	(0.030, 1.948, 67.8)	(0.030, 1.947, 39.6)	(0.030, 1.950, 26.4)	(0.030, 1.954, 99.0)	(0.030, 1.947, 68.1)	(0.030, 1.946, 39.6)	(0.030, 1.951, 26.4)
	1.2	0.18	(0.030, 1.957, 45.9)	(0.030, 1.948, 30.3)	(0.065, 2.303, 17.1)	(0.125, 2.536, 10.6)	(0.030, 1.954, 46.9)	(0.030, 1.947, 30.4)	(0.065, 2.303, 17.1)	(0.125, 2.535, 10.6)
	1.5	0.225	(0.055, 2.271, 15.4)	(0.130, 2.616, 9.5)	(0.265, 2.799, 4.9)	(0.400, 2.855, 3.0)	(0.070, 2.385, 15.5)	(0.130, 2.615, 9.5)	(0.265, 2.798, 4.9)	(0.400, 2.855, 3.0)
	2	0.3	(0.190, 2.824, 6.1)	(0.290, 2.899, 3.7)	(0.590, 2.991, 1.9)	(0.875, 2.979, 1.2)	(0.200, 2.839, 6.2)	(0.280, 2.887, 3.7)	(0.605, 2.994, 1.9)	(0.870, 2.977, 1.2)
0.2	1.1	0.22	(0.030, 1.947, 82.1)	(0.030, 1.941, 56.1)	(0.030, 1.937, 32.5)	(0.050, 2.169, 21.0)	(0.030, 1.947, 82.5)	(0.030, 1.940, 56.2)	(0.030, 1.939, 32.5)	(0.055, 2.215, 21.2)
	1.2	0.24	(0.030, 1.947, 37.5)	(0.035, 2.020, 24.7)	(0.090, 2.422, 13.5)	(0.175, 2.625, 8.3)	(0.030, 1.947, 37.6)	(0.035, 2.019, 24.7)	(0.090, 2.421, 13.5)	(0.175, 2.625, 8.3)
	1.5	0.3	(0.100, 2.520, 12.1)	(0.165, 2.672, 7.4)	(0.325, 2.816, 3.8)	(0.560, 2.881, 2.3)	(0.100, 2.518, 12.1)	(0.165, 2.671, 7.4)	(0.335, 2.823, 3.8)	(0.560, 2.881, 2.3)
	2	0.4	(0.245, 2.853, 4.7)	(0.370, 2.913, 2.8)	(0.730, 2.966, 1.4)	(0.910, 2.936, 1.0)	(0.230, 2.828, 4.7)	(0.370, 2.911, 2.8)	(0.730, 2.965, 1.4)	(0.910, 2.935, 1.0)

the RL properties as we have seen before). In any case, the upper-sided PEWMA chart with “continuousify” does not detect any out-of-control situation as it also visible in the control chart plotted in Figure 3.

Table 5: Example (printed circuit boards) of an upper-sided PEWMA chart with “continuousify”

Phase I					Phase II				
i	X_i	X_i^*	Z_i	Z_i^*	i	X_i	X_i^*	Z_i	Z_i^*
1	21	21.021	19.933	19.938	25	16	15.985	18.933	18.930
2	24	24.100	20.747	20.770	26	18	17.944	18.747	18.733
3	16	15.935	19.797	19.803	27	12	12.039	17.397	17.394
4	12	12.107	18.238	18.264	28	15	15.214	16.918	16.958
5	15	15.075	17.590	17.626	29	24	23.927	18.334	18.352
6	28	27.971	19.672	19.695	30	21	20.954	18.867	18.872
7	20	20.077	19.738	19.771	31	28	28.119	20.694	20.722
8	31	31.184	21.990	22.054	32	20	20.224	20.555	20.622
9	25	25.211	22.592	22.685	33	25	25.285	21.444	21.555
10	20	19.975	22.074	22.143	34	19	19.090	20.955	21.062
11	24	23.816	22.459	22.478	35	18	17.840	20.364	20.417
12	16	15.958	21.167	21.174	36	21	21.023	20.491	20.538
13	19	19.210	20.734	20.781	37	16	15.914	19.593	19.613
14	10	10.016	18.587	18.628	38	22	22.238	20.074	20.138
15	17	17.006	18.270	18.304	39	19	19.022	19.860	19.915
16	13	12.868	17.216	17.217	40	12	12.179	18.288	18.368
17	22	21.881	18.173	18.150	41	14	13.880	17.430	17.470
18	18	18.171	18.138	18.154	42	9	9.251	15.744	15.827
19	30	29.972	20.510	20.517	43	16	16.051	15.795	15.871
20	24	23.995	21.208	21.213	44	21	20.993	16.836	16.896
21	16	15.969	20.167	20.164					
22	19	18.761	19.933	19.884					
23	17	17.018	19.347	19.311					
24	15	15.062	18.477	18.461					

4.2 Example of an upper-sided BEWMA chart with “continuousify”

This example is also based on the data provided in Chapter 7 of Montgomery (2013) (Tables 7.2 and 7.3). In these tables the author provided the number of nonconforming frozen orange juice concentrate 6-oz cardboard cans in samples of $n = 50$ cans. This data set has been divided into two subsets: the first 24 samples are used as a Phase I data set and the remaining 40 samples are used as a Phase II data set (see column X_i in Table 6).

Using the Phase I data, the estimate of the in-control proportion of nonconforming cans is $\hat{p}_0 = \frac{133}{24 \times 50} = 0.1108$. Using Table 4 for $p_0 = 0.1$, $\tau = 1.2$ (20%

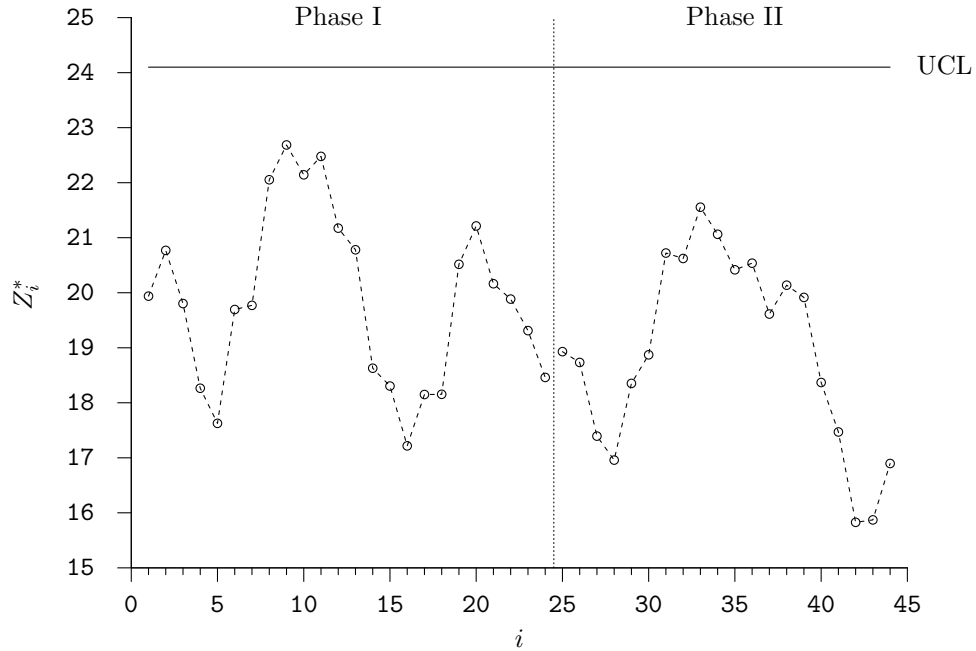


Figure 3: Example (printed circuit boards) of an upper-sided PEWMA chart with “continuousify”

increase), $\sigma = 0.125$ and $n = 50$, the optimal values for λ^* and K^* are 0.05 and 2.196, respectively. Therefore, the upper control limit UCL^* of the upper-sided BEWMA chart with the “continuousify” method is equal to

$$UCL^* = 50 \times 0.1108 + 2.196 \times \sqrt{\frac{0.05 \times (50 \times 0.1108(1 - 0.1108) + 0.125^2)}{2 - 0.05}} = 6.322.$$

Note again that, without the “continuousify” method (i.e. $\sigma = 0$), this upper control limit would have been $UCL = 6.320$ which is almost the same as for the with “continuousify” approach.

In addition to the number of nonconforming cans X_i , Table 6 also lists the values of X_i^* , Z_i (based on X_i) and Z_i^* for Phases I and II. As for the previous example, these Phases have been treated separately with initial values $Z_0 = Z_0^* = 50 \times 0.1108 = 5.54$. As it can be seen the values of Z_i (without “continuousify”) are different but they are nevertheless very close to those of Z_i^* (with “continuousify”). One more time, this highlights the fact that the “continuousify” technique has a very small impact in the computation of the EWMA statistic itself along with a positive impact in the computation of the RL properties). The upper-sided EWMA np chart with “continuousify” does not detect an out-of-control situation as it can be seen in the control chart plotted in Figure 4.

Table 6: Example (orange juice) of an upper-sided BEWMA chart with “continuousify”

Phase I					Phase II				
i	X_i	X_i^*	Z_i	Z_i^*	i	X_i	X_i^*	Z_i	Z_i^*
1	9	8.865	5.715	5.708	25	8	8.067	5.665	5.668
2	6	5.923	5.729	5.719	26	7	7.034	5.731	5.736
3	12	11.895	6.042	6.027	27	5	4.970	5.695	5.698
4	5	5.242	5.990	5.988	28	6	5.906	5.710	5.708
5	6	5.918	5.991	5.985	29	4	3.919	5.625	5.619
6	4	4.052	5.891	5.888	30	5	4.930	5.593	5.584
7	6	5.979	5.897	5.893	31	2	1.975	5.414	5.404
8	3	3.001	5.752	5.748	32	3	2.694	5.293	5.268
9	7	6.811	5.814	5.801	33	4	4.013	5.228	5.206
10	6	6.052	5.824	5.814	34	7	7.009	5.317	5.296
11	2	2.026	5.632	5.624	35	6	6.009	5.351	5.331
12	4	3.941	5.551	5.540	36	5	5.120	5.334	5.321
13	3	3.012	5.423	5.414	37	5	5.165	5.317	5.313
14	6	5.809	5.452	5.434	38	3	3.075	5.201	5.201
15	5	4.725	5.429	5.398	39	7	6.823	5.291	5.282
16	4	3.718	5.358	5.314	40	9	8.985	5.476	5.467
17	8	7.953	5.490	5.446	41	6	5.916	5.503	5.490
18	5	5.031	5.466	5.425	42	10	10.185	5.727	5.725
19	6	6.027	5.492	5.455	43	4	3.958	5.641	5.636
20	7	6.955	5.568	5.530	44	3	2.815	5.509	5.495
21	5	4.963	5.539	5.502	45	5	5.053	5.484	5.473
22	6	5.793	5.562	5.517	46	8	7.948	5.609	5.597
23	3	2.857	5.434	5.384	47	11	10.739	5.879	5.854
24	5	4.885	5.413	5.359	48	9	8.888	6.035	6.006
					49	7	7.057	6.083	6.058
					50	3	3.122	5.929	5.911
					51	5	4.925	5.883	5.862
					52	2	2.085	5.688	5.673
					53	1	0.868	5.454	5.433
					54	4	4.122	5.381	5.367
					55	5	4.676	5.362	5.333
					56	3	2.966	5.244	5.215
					57	7	7.192	5.332	5.313
					58	6	6.092	5.365	5.352
					59	4	3.936	5.297	5.282
					60	4	4.080	5.232	5.221
					61	6	6.135	5.271	5.267
					62	8	7.897	5.407	5.399
					63	5	5.056	5.387	5.381
					64	6	6.106	5.417	5.418

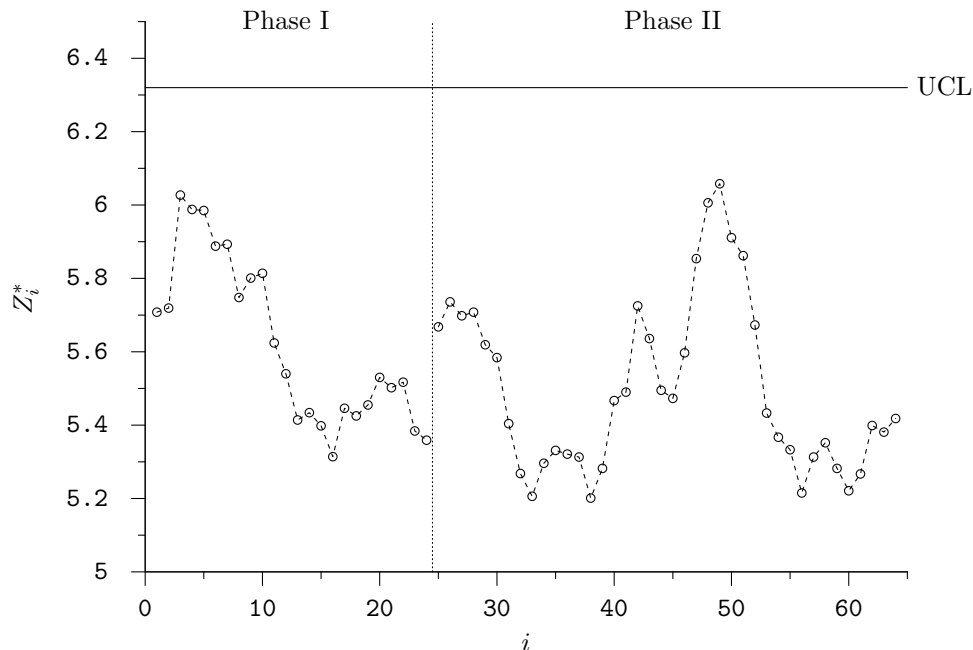


Figure 4: Example (orange juice) of an upper-sided BEWMA chart with “continuousify”

5 Conclusions

In this paper, we propose a new method to obtain reliable RL properties of an EWMA type chart for count data. Due to the discrete nature of count data, the traditional approaches that are used to obtain the exact RL properties of an EWMA chart show an unstable (and thus unreliable) performance. Of course the problem can be partially confronted by the use of Monte Carlo simulation. However, this approach can be very time consuming when the need is to appropriately design the chart (i.e. determine the optimal values for its chart’s constants).

The main findings from our study are i) the “continuousify” technique is a simple approach that allows to compute the RL properties of any attribute EWMA type control charts in a reliable way by obtaining stable values no matter the number of sub-intervals $m > 100$ used in the Markov chain method. Even for $m = 100$, the results are very stable and reliable and, obviously, less computational effort is needed. ii) the ARL values obtained using the “continuousify” method are negligibly larger than the ones obtained without the “continuousify” method, iii) the choice of the “continuousify” parameter σ has a negligible influence on the evaluation of the RL properties as long as this one is not too small nor too big. A good compromise seems to be a value $\sigma \in [0.1, 0.2]$, iv) the fact that the ARL values obtained using the “continuousify” method are stable makes possible to optimize any kind of EWMA chart for discrete distributions

in an efficient way. Finally, a comparison with the recent ‘‘Splitting Markov Chain’’ approach proposed by Morais and Knoth (2020) has shown that our ‘‘continuousify’’ method performs in a similar way in the case of the PEWMA control chart.

This method can be used for any discrete distributions like the Zero-Inflated Poisson, Binomial or Negative Binomial ones. Moreover, other smoothing kernels (in place of the normal kernel used in this paper) can also be investigated like the Epanechnikov, Biweight and Triweight (see Wand and Jones (1994)).

Appendix

By definition, using (1), we have

$$E(X^*) = \int_{-\infty}^{+\infty} x \left(\sum_{\omega \in \Omega} f_X(\omega|\boldsymbol{\theta}) f_N(x|\omega, \sigma) \right) dx.$$

Exchanging the integral and the sum gives

$$\begin{aligned} E(X^*) &= \sum_{\omega \in \Omega} \underbrace{\int_{-\infty}^{+\infty} x f_N(x|\omega, \sigma) dx}_{\omega} f_X(\omega|\boldsymbol{\theta}) \\ &= \sum_{\omega \in \Omega} \omega f_X(\omega|\boldsymbol{\theta}) = E(X). \end{aligned}$$

Using the same approach, we have

$$\begin{aligned} E(X^{*2}) &= \sum_{\omega \in \Omega} \underbrace{\int_{-\infty}^{+\infty} x^2 f_N(x|\omega, \sigma) dx}_{\omega^2 + \sigma^2} f_X(\omega|\boldsymbol{\theta}) \\ &= \sum_{\omega \in \Omega} \omega^2 f_X(\omega|\boldsymbol{\theta}) + \sigma^2 \underbrace{\sum_{\omega \in \Omega} f_X(\omega|\boldsymbol{\theta})}_1 = E(X^2) + \sigma^2, \end{aligned}$$

and since $E(X^*) = E(X)$ we also have $V(X^*) = V(X) + \sigma^2$.

References

- V. Alevizakos and C. Koukouvinos. A Double Exponentially Weighted Moving Average Control Chart for Monitoring COM-Poisson Attributes. *Quality and Reliability Engineering International*, 35(7):2130–2151, 2019.
- W. Arshad, N. Abbas, M. Riaz, and Z. Hussain. Simultaneous Use of Runs Rules and Auxiliary Information with Exponentially Weighted Moving Average Control Charts. *Quality and Reliability Engineering International*, 33(2): 323–336, 2017.
- M. Aslam, N. Khan, and C.H. Jun. A Hybrid Exponentially Weighted Moving Average Chart for COM-Poisson Distribution. *Transactions of the Institute of Measurement and Control*, 40(2):456–461, 2018.

- C. Bilen, A. Khan, and W. Chattinnawat. Dual-Monitoring Scheme for Multivariate Autocorrelated Cascade Processes with EWMA and MEWMA Charts. *Quality Technology & Quantitative Management*, 14(2):156–177, 2017.
- C.M. Borrór, C.W. Champ, and S.E. Rigdon. Poisson EWMA Control Charts. *Journal of Quality Technology*, 30(4):352–361, 1998.
- D. Brook and D.A. Evans. An Approach to the Probability Distribution of CUSUM Run Length. *Biometrika*, 59(3):539–549, 1972.
- F.F. Gan. Monitoring Poisson Observations using Modified Exponentially Weighted Moving Average Control Charts. *Communications in Statistics – Simulation and Computation*, 19(1):103–124, 1990a.
- F.F. Gan. Monitoring Observations Generated from a Binomial Distribution using Modified Exponentially Weighted Moving Average Control Chart. *Journal of Statistical Computation and Simulation*, 37(1-2):45–60, 1990b.
- S. Haridy, M.A. Rahim, S.Z. Selim, Z. Wu, and J.C. Benneyan. EWMA Chart with Curtailment for Monitoring Fraction Nonconforming. *Quality Technology & Quantitative Management*, 14(4):412–428, 2017.
- M.B.C. Khoo, P. Castagliola, J.Y. Liew, W.L. Teoh, and P.E. Maravelakis. A Study on EWMA Charts with Runs Rules – the Markov Chain Approach. *Communications in Statistics – Theory and Methods*, 45(14):4156–4180, 2016.
- G. Latouche and V. Ramaswami. *Introduction to Matrix Analytic Methods in Stochastic Modeling*. ASA-SIAM, Philadelphia, 1999.
- S.L. Lu and C.J. Huang. Statistically Constrained Economic Design of Maximum Double EWMA Control Charts Based on Loss Functions. *Quality Technology & Quantitative Management*, 14(3):280–295, 2017.
- P.E. Maravelakis, P. Castagliola, and M.B.C. Khoo. Run Length Properties of Run Rules EWMA Chart using Integral Equations. *Quality Technology & Quantitative Management*, 16(2):129–139, 2019.
- D.C. Montgomery. *Introduction to Statistical Quality Control*. John Wiley & Sons, 111 River Street, Hoboken, NJ 07030-5774, USA, 7 edition, 2013.
- M.C. Morais and S. Knoth. Improving the ARL Profile and the Accuracy of its Calculation for Poisson EWMA Charts. *Quality and Reliability Engineering International*, 36(3):876–889, 2020.
- M.F. Neuts. *Matrix-Geometric Solutions in Stochastic Models: an Algorithmic Approach*. Dover Publications Inc, New York, 1981.
- T. Perdikis, S. Psarakis, P. Castagliola, and P.E. Maravelakis. An EWMA Signed Ranks Control Chart with Reliable Run Length Performances. *Quality and Reliability Engineering International*, 37(3):1266–1284, 2021.
- I.A. Raji, N. Abbas, and M. Riaz. On Designing a Robust Double Exponentially Weighted Moving Average Control Chart for Process Monitoring. *Transactions of the Institute of Measurement and Control*, 40(15):4253–4265, 2018.

- M. Riaz and S.A. Abbasi. Nonparametric Double EWMA Control Chart for Process Monitoring. *Revista Colombiana de Estadística*, 39(2):167–184, 2016.
- S.W. Roberts. Control Chart Tests Based on Geometric Moving Averages. *Technometrics*, 1(3):239–250, 1959.
- A. Saghir and Z. Lin. A Flexible and Generalized Exponentially Weighted Moving Average Control Chart for Count Data. *Quality and Reliability Engineering International*, 30(8):1427–1443, 2014.
- S.E. Somerville, D.C. Montgomery, and G.C. Runger. Filtering and Smoothing Methods for Mixed Particle Count Distributions. *International Journal of Production Research*, 40(13):2991–3013, 2002.
- J.L. Szarka and W.H Woodall. A Review and Perspective on Surveillance of Bernoulli Processes. *Quality and Reliability Engineering International*, 27(6):735–752, 2011.
- A.A. Tang, P. Castagliola, J.S. Sun, and X.L. Hu. Optimal Design of the Adaptive EWMA Chart for the Mean Based on Median Run Length and Expected Median Run Length. *Quality Technology & Quantitative Management*, 16(4):439–458, 2019.
- M.P. Wand and M.C. Jones. *Kernel Smoothing*. CRC press, 1994.
- S. Wu, P. Castagliola, and G. Celano. A Distribution-Free EWMA Control Chart for Monitoring Time-Between-Events-and-Amplitude Data. *Journal of Applied Statistics*, 2020. doi: 10.1080/02664763.2020.1729347.
- A.B. Yeh, R.N. Mcgrath, M.A. Sembower, and Q. Shen. EWMA Control Charts for Monitoring High-Yield Processes Based on Non-Transformed Observations. *International Journal of Production Research*, 46(20):5679–5699, 2008.
- L. Zhang, K. Govindaraju, C.D. Lai, and M.S. Bebbington. Poisson DEWMA Control Chart. *Communications in Statistics-Simulation and Computation*, 32(4):1265–1283, 2003.
- I.M. Zwetsloot, M. Schoonhoven, and R.J.M.M. Does. Robust Point Location Estimators for the EWMA Control Chart. *Quality Technology & Quantitative Management*, 13(1):29–38, 2016.